



Metabolic homeostasis and growth in abiotic cells

Amir Akbari^a and Bernhard O. Palsson^{a,b,1}

Edited by Jens Nielsen, BioInnovation Institute, Copenhagen, Denmark; received January 12, 2023; accepted March 27, 2023

Metabolism constitutes the core chemistry of life. How it began on the early Earth and whether it had a cellular origin are still uncertain. A leading hypothesis for life's origins postulates that metabolism arose from geochemical CO₂-fixing pathways, driven by inorganic catalysts and energy sources, long before enzymes or genes existed. The acetyl-CoA pathway and the reductive tricarboxylic acid cycle are considered ancient reaction networks that hold relics of early carbon-fixing pathways. Although transition metals can promote many steps of these pathways, whether they form a functional metabolic network in abiotic cells has not been demonstrated. Here, we formulate a nonenzymatic carbon-fixing network from these pathways and determine its functional feasibility in abiotic cells by imposing fundamental physicochemical constraints. Using first principles, we show that abiotic cells can sustain a steady carbon-fixing cycle that performs a systemic function over a relatively narrow range of conditions. Furthermore, we find that in all feasible steady states, the operation of the cycle elevates the osmotic pressure, leading to volume expansion. These results suggest that achieving homeostatic metabolic states under prebiotic conditions was possible, but challenging, and volume growth was a fundamental property of early metabolism.

origin of metabolism | carbon-fixing cycles | alkaline hydrothermal vents | metabolic homeostasis | emergent properties

How life originated on a lifeless planet from nothing but a few inorganic precursors is a fundamental question in biology. Ever since Oparin's primordial soup theory (1), two major hypotheses have been developed to address this question: one centered around information and the other around chemical self-organization. Which was more fundamental to the emergence of life is still debated (2); that metabolism and self-organization play a prominent role in extant biology is not. Interestingly, phylogenetic studies of all domains of life trace biochemistry to an ancient autotrophic network at the core of metabolism (3). These studies point to a core network that would have been anaerobic (3), phosphate-free (4), and reliant on simple carbon and energy sources (3).

Recent theories of life's origins posit that metabolism originated from a geochemical protometabolism that predated enzymes and genes (2, 5). They consider early metabolic pathways that were thermodynamically favorable and promoted by naturally occurring catalysts (e.g., transition metals) and reducing compounds (e.g., H₂, FeS) (6). Alkaline hydrothermal vents (AHVs) in the Hadean ocean are believed to have harbored these early pathways, providing inorganic catalysts, simple carbon sources, and a continuous supply of energy and reducing power (5) (Fig. 1A). The steep redox and pH gradients in AHVs would have been sufficient to drive energy and carbon metabolism (8). Experimental evidence suggests that transition metals and inorganic reducing agents can promote several core metabolic pathways (10–15), corroborating AHV theories. However, whether a self-sustaining network comprising a series of core metabolic reactions could have spontaneously arisen and operated nonenzymatically under hydrothermal-vent conditions is still unclear.

At the origin of metabolism, boundary structures may have been required to i) generate concentration gradients between compartments and their surroundings, providing a continuous supply of energy and material to maintain stable far-from-equilibrium states (16) and ii) create a barrier to limit diffusive loss of metabolic products (17). Before the advent of enzymes, abiotic cellular structures could have facilitated the inception of the first self-amplifying metabolic networks on Earth (18, 19). However, the lack of selective transporters, efficient catalysts, and evolutionarily optimized energy-coupling mechanisms (e.g., electron bifurcation) in such compartments could also have limited the continued operation of these networks. Therefore, whether abiotic cells can sustain stable carbon-fixing cycles without enzymes is to be demonstrated. In this regard, first-principle analyses of abiotic systems that are consistent with established chemistries of nonenzymatic metabolism could elucidate the key factors constraining the emergence of metabolism.

Significance

Metabolism is believed to have emerged from ancient autotrophic pathways fueled by volcanic gases as carbon and energy sources. Variants of these pathways remain in modern autotrophs in the deepest branches of the tree of life. The energy metabolism of modern autotrophs resembles the geological interactions of H₂ and CO₂ in hydrothermal vents, pointing to a metabolic origin of biochemistry at the interface of the lithosphere and hydrosphere. Here, we demonstrate the feasibility of self-sustaining, self-amplifying CO₂ fixation by H₂ in hydrothermal pores using a first-principle approach that is consistent with physicochemical constraints and chemistry of prebiotic carbon fixation. We identify the conditions for the emergence of metabolism on the early Earth, revealing the fundamental nature of biological carbon fixation.

Author affiliations: ^aDepartment of Bioengineering, University of California San Diego, La Jolla, CA 92093; and ^bNovo Nordisk Foundation Center for Biosustainability, Technical University of Denmark, Building 220, Kemitorvet, 2800 Kongens Lyngby, Denmark

Author contributions: A.A. designed research; A.A. performed research; A.A. analyzed data; B.O.P. provided resources and supervision; and A.A. and B.O.P. wrote the paper.

The authors declare no competing interest.

This article is a PNAS Direct Submission.

Copyright © 2023 the Author(s). Published by PNAS. This open access article is distributed under Creative Commons Attribution-NonCommercial-NoDerivatives License 4.0 (CC BY-NC-ND).

¹To whom correspondence may be addressed. Email: palsson@ucsd.edu.

This article contains supporting information online at <http://www.pnas.org/lookup/suppl/doi:10.1073/pnas.2300687120/-/DCSupplemental>.

Published May 1, 2023.

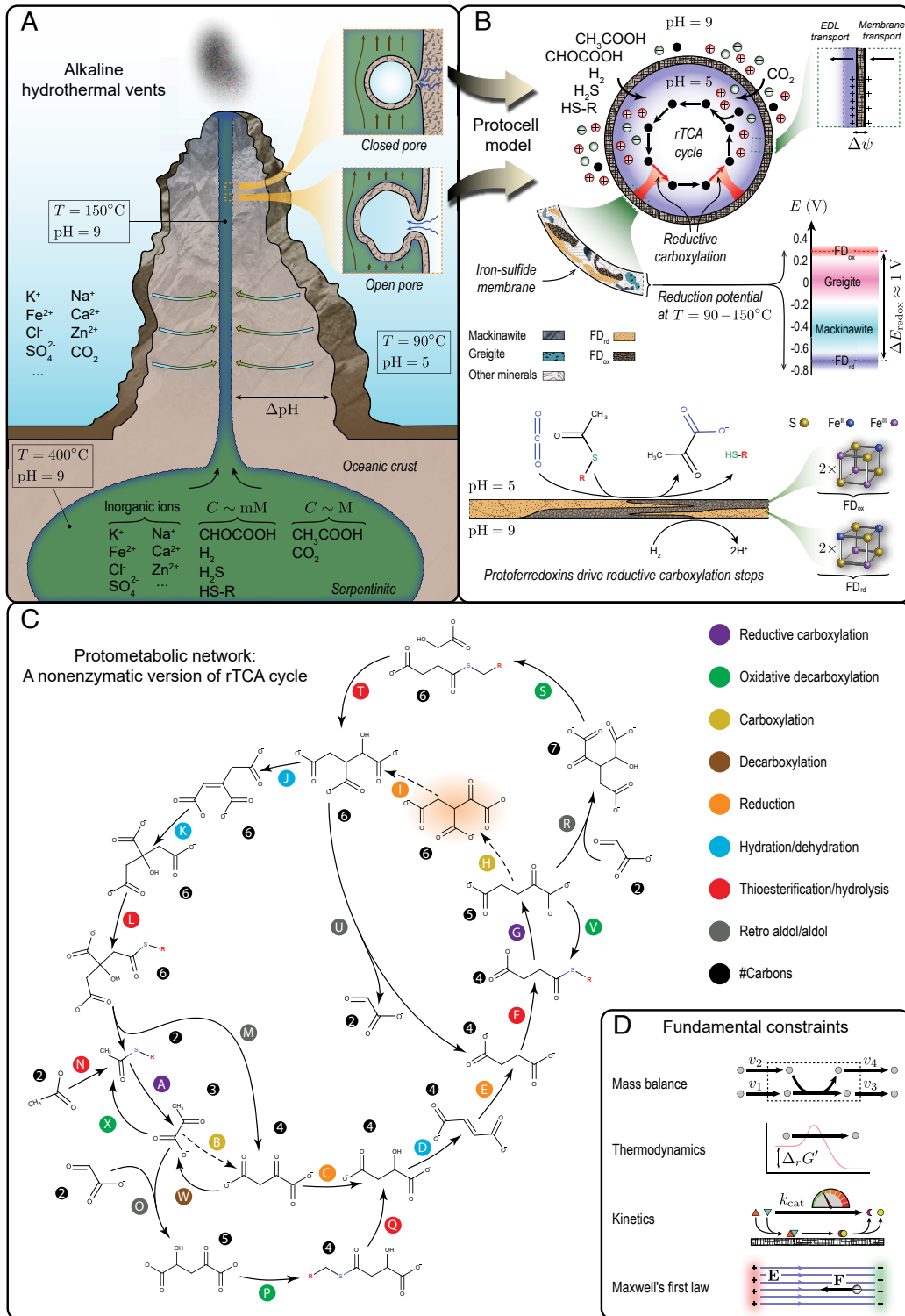


Fig. 1. Emergence of first metabolic cycles from abiotic geochemical processes. (A) Deep-sea alkaline hydrothermal vents in the Hadean ocean were ideal environments from which metabolic pathways could spontaneously arise (5, 7). Hydrothermal fluids formed by serpentinization would have been alkaline and rich in naturally occurring catalysts (e.g., metal ions, minerals) and reducing compounds (e.g., H_2 , H_2S , FeS), providing the necessary ingredients for the emergence of metabolic networks. Thin-walled micropores made of iron sulfides forming along vent conduits, such as those shown in the inset (SI Appendix, Fig. S2), provide an interface between alkaline hydrothermal fluids and acidic ocean (8). Redox and pH gradients across such inorganic barriers could have powered the synthesis of first organic molecules. (B) Protocell model with an iron-sulfide membrane simulates the formation of first metabolic cycles in vent micropores. All metabolic reactions beside carbon-fixing steps are catalyzed by transition metals in aqueous or solid phase dispersed inside the protocell in an acidic environment. Carbon-fixation reactions are catalyzed by protoferredoxins on the inner surface of the membrane. Protoferredoxins could have formed in the presence of iron and sulfur ions under hydrothermal conditions (8, 9). Reduced (FD_{red}) and oxidized (FD_{ox}) protoferredoxins would have had similar crystal structures to hydrothermal mineral redox couples (e.g., mackinawite/greigite), providing a sufficiently large redox potential to drive carbon fixation (8). Reduced protoferredoxins consumed by carbon-fixation steps are regenerated on the outer surface of the membrane in an alkaline environment using H_2 as a reducing agent. (C) Phosphate-free protometabolic network examined in this work comprising a nonenzymatic version of the rTCA cycle, containing all its intermediates except oxalosuccinate (highlighted in red). Dashed arrows indicate the corresponding enzymatic steps that are not included in the network. Thioesterification steps are driven by a simple hydrothermal thiol HS-R that could have been synthesized in sulfide-rich environments (8) with R a hypothetical substituent. (D) Fundamental constraints of the protocell model (see SI Appendix for details).

Results

Protocell Model of Hydrothermal-Vent Pores. Biology is a science of emergence. Therefore, we must show that if all components of abiotic cells work together collectively, a functioning system capable of reaching steady states will emerge. Thus, we developed a protocell model (Fig. 1*B*) to simulate AHV conditions on the early Earth and answer whether AHV micropores could have harbored nonenzymatic autotrophic pathways using first principles (*SI Appendix, Model Description*). In this protocell, the membrane is made of iron sulfides, a fraction of which are protoferredoxins. The membrane separates an acidic interior from alkaline surroundings. This pH gradient induces a positive membrane potential. It alleviates the dissipation of metabolic products (20) and provides the energy required for carbon fixation—a primitive energy-coupling mechanism mediated by protoferredoxins independently of ATPase and proton pumps. Abiotic metabolic reactions occur inside the protocell, and compounds cross the membrane unselectively via passive diffusion.

We began by assessing candidate abiotic chemical networks at the origin of metabolism, focusing on carbon assimilation in modern autotrophs. From the six known CO₂-fixing pathways (2), the reductive tricarboxylic acid (rTCA) cycle is considered the most ancient autocatalytic and a primordial core network (21). It contains the five universal precursors of metabolism (*SI Appendix, Fig. S3*); all its intermediates but cofactors are phosphate-free; and several of its reactions can be promoted by transition metals (13). Thus, we reconstructed a protometabolic network (Fig. 1*C*) based on the rTCA cycle to represent the first carbon-fixing cycles from which metabolism originated (*SI Appendix, First Carbon-Fixing Cycles at the Origin of Metabolism*). This network is cyclic and phosphate-free, only requiring inorganic cofactors and catalysts. Except for succinate reductive carboxylation, all its steps are derived from experimentally demonstrated nonenzymatic reactions or their close analogues (11, 13, 14, 22–24). Neutral carboxylation steps from the enzymatic rTCA cycle (Fig. 1*C*, steps B and H) are not included in the network. These steps have not been reproduced nonenzymatically and are unlikely to proceed without evolutionarily tuned cofactors like ATP. Hence, they are bypassed through aldol and decarboxylation reactions. Acetate, glyoxylate, and CO₂ are the carbon sources: Glyoxylate drives the foregoing bypass pathways, while acetate amplifies the cycle.

Were there plausible conditions under which carbon fixation was feasible subject to the restrictions of enzyme-free metabolism and fundamental physicochemical constraints? Could abiotic cells have operated on simple carbon and energy sources, while exhibiting fundamental characteristics of living cells, such as growth and homeostasis? Answering these questions is a challenging task, requiring a systems-level analysis of constrained reaction–diffusion problems. To address these questions, we formulated a dynamic system, accounting for the fundamental constraints (20, 25) arising from mass conservation, thermodynamics, kinetics, and Maxwell's first law (Fig. 1*D*). By studying the steady-state solutions and stability of this system, we quantified the feasibility and homeostatic states of the proposed protometabolism.

Emergence of Metabolic Homeostasis and Growth. The turnover number and membrane potential are key parameters that encapsulate the restrictions of nonenzymatic metabolism. Low turnover numbers characterize inorganic-catalyst efficiencies, while positive membrane potentials are required to lower metabolic-product dissipation through semipermeable inorganic membranes. Remarkably, we identified a restricted stability region in this parameter space where stable steady states that

satisfy the fundamental constraints of the early Earth can be achieved (Fig. 2*A*). These states represent abiotic metabolic homeostasis, where a complete-cycle flux can be sustained.

The dynamics of the protometabolic network are affected the most by physicochemical constraints near the stability-region boundaries. The stability region is bounded at low and high membrane potentials but unbounded in turnover numbers. These boundaries correspond to “critical” points where multiple steady states coexist. At these critical points, steady states become unstable and solution branches bifurcate. The boundary at low membrane potentials corresponds to turning points. Here, there is a minimum membrane potential at a fixed turnover number below which no steady-state solution associated with a complete-cycle flux exists. Below this minimum limit, the membrane potential is not sufficiently strong to create a large acetate concentration at the network entry to drive a flux through the entire cycle (Fig. 2*C*). In contrast, the boundary at high membrane potentials corresponds to branch points, where steady-state solutions associated with a complete-cycle flux at a fixed turnover number can be continued along two distinct directions, although these solutions are unstable. Overall, the protocell model exemplifies evolvable systems with coexisting stable and unstable states that are amenable to nongenetic selection (27, 28). In these systems, physicochemical properties that yield the most stable states are those that are selected for in long evolutionary processes.

Achievable parameter values under hydrothermal conditions determine part of the stability region that is relevant to the emergence of first metabolic cycles. For example, turnover numbers furnished by hydrothermal minerals would likely have been significantly lower than those of enzymes. Similarly, membrane potentials that were larger in magnitude than those of modern cells would unlikely have been attained due to thermodynamic and stability constraints (20). Moreover, concentrations should have remained above a minimum level to support metabolic reactions. Accounting for all these restrictions, we qualitatively identified a feasible region (Fig. 2*A*, area enclosed by red lines) that allows a self-sustaining rTCA cycle to emerge. The resulting parameter ranges are relatively narrow, highlighting the underlying challenges of cyclic carbon fixation on the early Earth.

The feasibility of carbon-fixing pathways is largely determined by their energetics. The protometabolic network that we reconstructed has several thermodynamic bottlenecks under standard conditions (Fig. 2*D*, blue arrows). To overcome these energy barriers, a large concentration differential must be generated between the reactants and products of uphill reactions. Moreover, all concentrations must remain above a minimum level to ensure that a stable flux passes through the entire cycle. To this end, the concentration and import flux of acetate at the network entry must be sufficiently large to compensate for the dissipation of the intermediates along the way. The concentration of the intermediates are distributed around the cycle accordingly to eliminate all the uphill reactions. Any given point inside the stability region corresponds to a complete-cycle flux (Fig. 2*B*) with no uphill reactions (Fig. 2*E*). The intermediates in the upper half of the cycle carry more negative charge than those in the lower half. Therefore, positive membrane potentials reduce the dissipation rates and amplify the fluxes and concentrations in the upper half more than in the lower half.

Our protocell model exhibits a growth-like characteristic once it attains a stable steady state, constantly converting substrates (carbon and energy sources) into organic products. Both substrates and products of the protometabolic network are negatively charged. Hence, positive membrane potentials enhance substrate import and alleviate product dissipation. The net effect is an

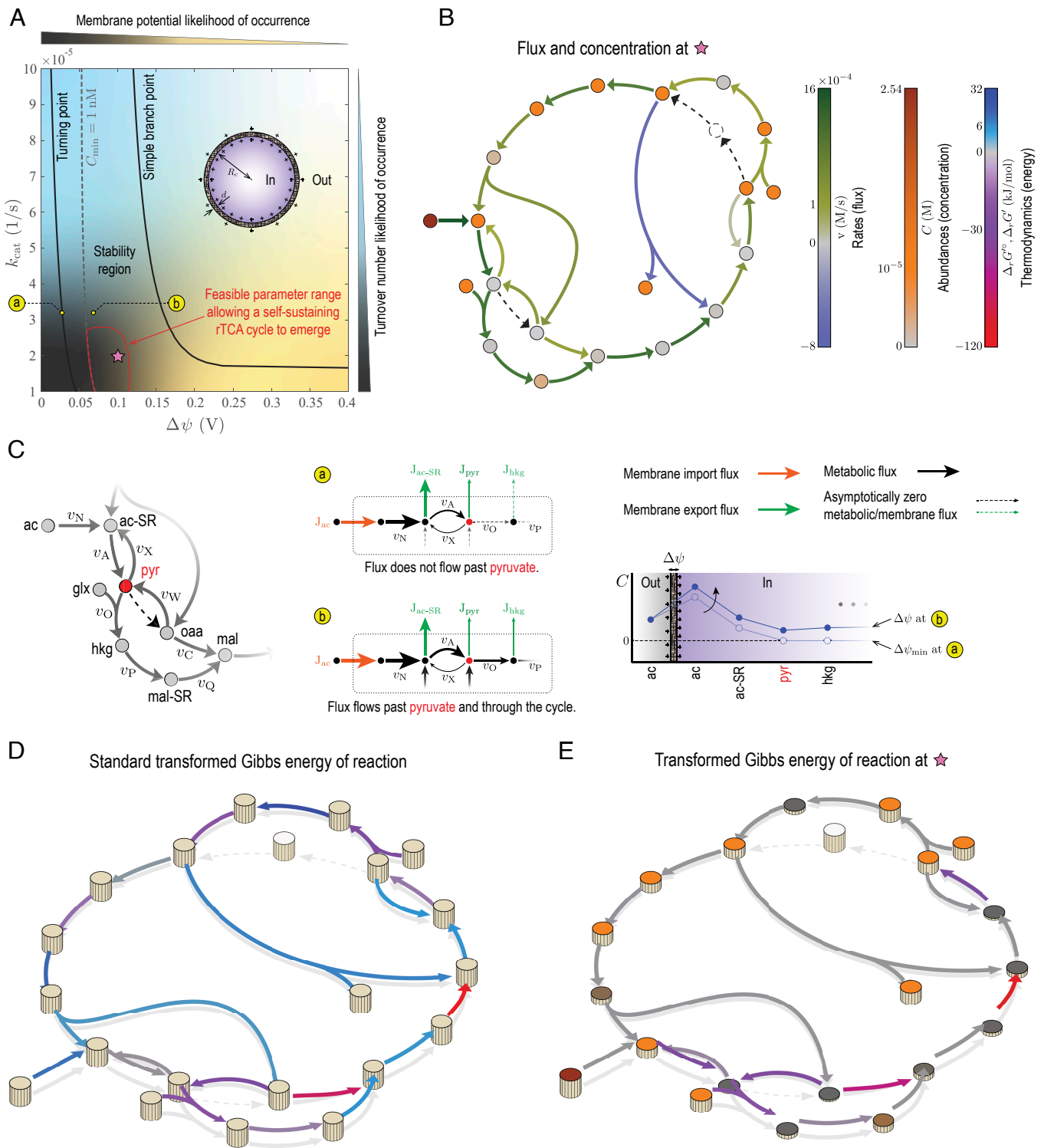


Fig. 2. Feasibility of first carbon-fixing cycles at the origin of metabolism. (A) Stability region of the rTCA cycle in Fig. 1C with respect to the turnover number k_{cat} and membrane potential $\Delta\psi$. The turnover number of all the steps in the network are identical (*SI Appendix, Kinetic Constraints*). Steady-state solutions of mass-balance equations are stable in the area confined by solid black lines, where solution branches bifurcate. The dashed line corresponds to a lower bound (1 nM) imposed on the minimum concentration of reactants in the network C_{min} , splitting the stability region into two subregions. The minimum concentration is less than the lower bound in the *Left* and more than the lower bound in the *Right* subregion. Generating large membrane potentials ($\Delta\psi \gtrsim 0.15$ V) in abiotic cells would have been unlikely due to thermodynamic limitations on charge densities that can be induced on mineral surfaces and stability constraints (20). Hydrothermal minerals would likely have furnished small turnover numbers ($k_{cat} \approx 10^{-5}$ 1/s) due to their poor catalytic efficiency. Given these restrictions, the region enclosed by red lines indicates parameter ranges that allow a self-sustaining rTCA cycle to operate. (B) Metabolic fluxes and concentrations at a point inside the stability region that represent likely conditions of hydrothermal vents in the Hadean ocean. (C) Distribution of metabolic fluxes and concentrations near the network entry, where acetate feeds into the rTCA cycle. A minimum membrane potential is required to sustain a stable flux through the entire cycle. Positive membrane potentials generate a large concentration gradient at the cycle entry by elevating the acetate concentration while minimizing the dissipation of downstream intermediates, thus driving a flux through all the thermodynamic bottlenecks. (D) Standard transformed Gibbs energy of reactions. (E) Transformed Gibbs energy of reactions at the same point as fluxes and concentrations in (B) are evaluated. Note that the transformed Gibbs energy determines the spontaneity of reactions when pH is a control parameter besides temperature and pressure (26), as is the case in this work. Model parameters are given in *SI Appendix, Table S3*.

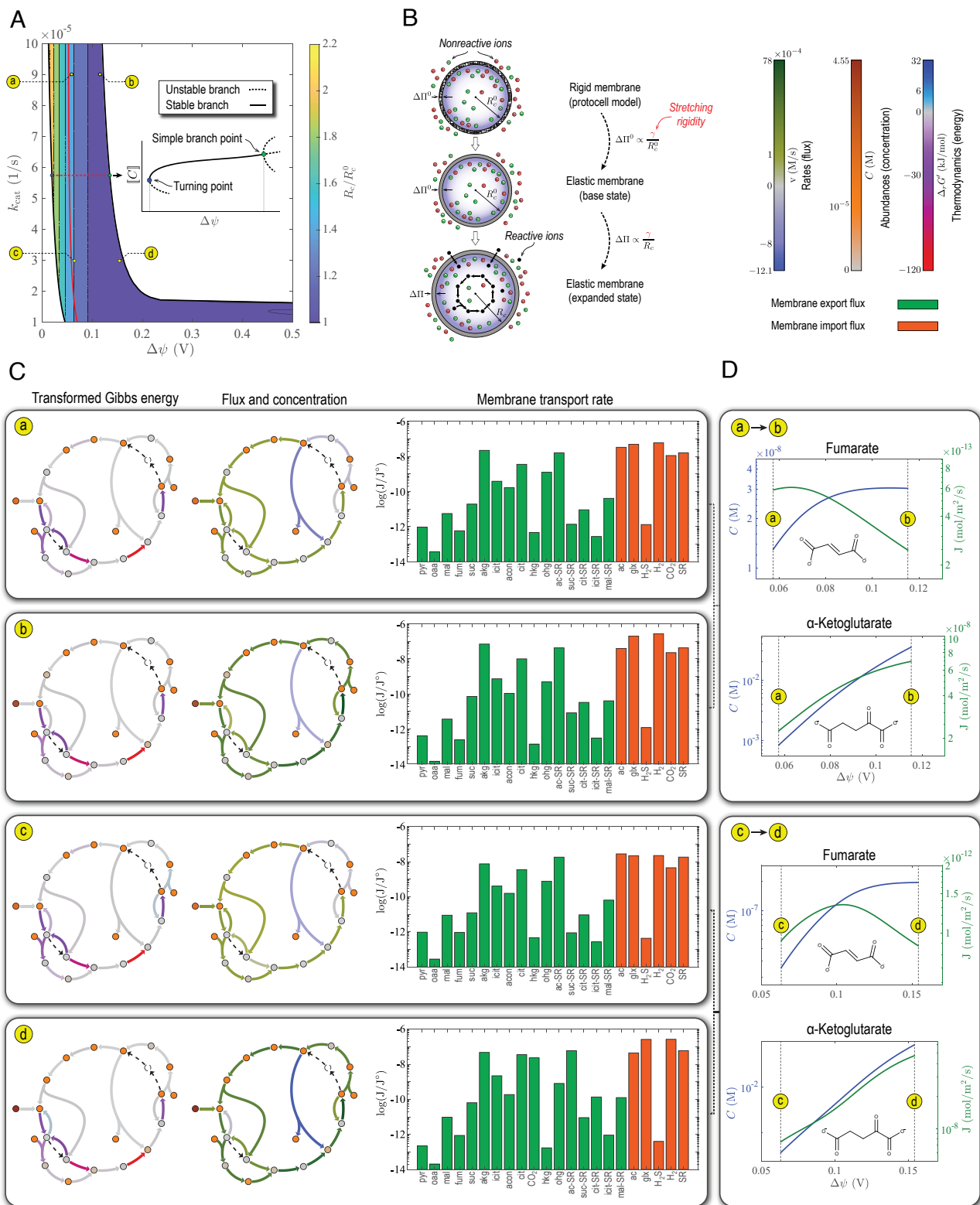


Fig. 3. Steady-state characteristics of first carbon-fixing cycles. (A) Volume expansion induced in the protocell by the osmotic pressure resulting from accumulation of the organic products of the rTCA cycle in Fig. 1C. Solid red line corresponds to a minimum-concentration lower bound imposed on steady-state concentrations (dashed line in Fig. 2A). In the *Inset*, $[C]$ denotes a solution norm used to represent branching diagrams. (B) Definition of volume expansion shown in (A). The membrane in the protocell model (Fig. 1B) used to characterize the steady states of the rTCA cycle is rigid. However, to estimate the volume expansion resulting from the operation of the protometabolic network, the radius of a protocell with an elastic membrane, containing steady-state concentrations of metabolic products from the protocell model (expanded state), is compared to that of another protocell with an elastic membrane in which only the inorganic ions of the early ocean are present (base state) (SI Appendix, Osmotic Pressure Drives Protocell Growth). The osmotic pressure differential in the first and second case is denoted $\Delta\Pi$ and $\Delta\Pi^0$ with R_c and R_c^0 the respective protocell radii. Both metabolic products and inorganic ions contribute to $\Delta\Pi$ in the first case, while inorganic ions alone generate $\Delta\Pi^0$ in the second case. The stretching rigidity γ of the membrane is the same in both cases. (C) Steady-state transformed Gibbs energy of reactions, metabolic fluxes, concentrations, and membrane transport rates at representative points along the boundaries of the stability region. Here, $J^0 = 1 \text{ mol/m}^2/\text{s}$ is a reference flux used to nondimensionalize the argument of the logarithm function. (D) Changes in the concentration and membrane transport rate of representative intermediates of the rTCA cycle induced by the membrane potential. Model parameters are given in SI Appendix, Table S3.

accumulation of more ions in the protocell and a higher osmotic pressure differential than if no metabolic reaction occurred. Overall, the protocell tends to expand as a result of abiotic metabolism. This is a general characteristic of the protometabolic network, irrespective of parameter values (Fig. 3 A and B).

Both turnover number and membrane potential enhance membrane transport rates and metabolic fluxes. However, the membrane potential has a stronger effect (Fig. 3C), making it the main driving force of metabolism and growth in the protocell model. Moreover, because rate laws and charge-related transport rates are nonlinear, increasing the membrane potential does not affect all the intermediates to the same degree. For example, increasing the membrane potential at large turnover numbers causes the protocell to accumulate and secrete α -ketoglutarate at a faster rate than other intermediates (e.g., fumarate) (Fig. 3D). α -ketoglutarate is a precursor for primordial synthesis of glutamate (29). Glutamate and cysteine in turn can chelate FeS crystals (9, 30), generating a feedback into the reductive carboxylation steps (SI Appendix, Fig. S5). Such positive feedbacks could have amplified first carbon-fixing cycles and underlain the evolutionary selection of physicochemical properties that were optimal for amino acid synthesis.

Discussion

Here, we demonstrated that iron-sulfide protocells could have harbored first carbon-fixing cycles using a first-principle and systems-level approach. These protocells could achieve a sustainable metabolic homeostasis in a narrow parameter range, supporting the hypothesis that, although challenging, cellular metabolism inevitably emerged from geochemical interactions of the early lithosphere and hydrosphere (28). Stable, self-amplifying carbon fixation was restricted by the membrane potential but unrestricted by the turnover number in our model. These results suggest that, at the origin of metabolism, evolution could have acted on turnover numbers unrestrictedly to improve fitness, maintaining the membrane potential within the tight bounds of physicochemical constraints. Our first-principle approach could guide future experimental designs to examine the compartmentalization of self-sustaining carbon-fixing networks, opening exciting directions in the coming years for 'systems' studies of life's metabolic origins.

1. A. I. Oparin, *The Origin of Life on the Earth* (Oliver & Boyd, Edinburgh & London, 1957).
2. K. B. Muchowska, S. J. Varma, J. Moran, Nonenzymatic metabolic reactions and life's origins. *Chem. Rev.* **120**, 7708–7744 (2020).
3. J. C. Xavier, W. Hordijk, S. Kauffman, M. Steel, W. F. Martin, Autocatalytic chemical networks at the origin of metabolism. *Proc. Royal Soc. B* **287**, 20192377 (2020).
4. J. E. Goldford, H. Hartman, T. F. Smith, D. Segrè, Remnants of an ancient metabolism without phosphate. *Cell* **168**, 1126–1134 (2017).
5. W. Martin, M. J. Russell, On the origin of biochemistry at an alkaline hydrothermal vent. *Philos. Trans. R. Soc. B* **362**, 1887–1926 (2007).
6. G. Wächtershäuser, Groundworks for an evolutionary biochemistry: The iron-sulphur world. *Prog. Biophys. Molec. Biol.* **58**, 85–201 (1992).
7. N. Lane, *The Vital Question: Energy, Evolution, and the Origins of Complex Life* (WW Norton & Company, 2015).
8. M. J. Russell, A. J. Hall, The emergence of life from iron monosulphide bubbles at a submarine hydrothermal redox and pH front. *J. Geol. Soc.* **154**, 377–402 (1997).
9. S. F. Jordan *et al.*, Spontaneous assembly of redox-active iron-sulfur clusters at low concentrations of cysteine. *Nat. Commun.* **12**, 1–14 (2021).
10. C. Huber, G. Wächtershäuser, Activated acetic acid by carbon fixation on (Fe, Ni)S under primordial conditions. *Science* **276**, 245–247 (1997).
11. G. D. Cody *et al.*, Primordial carbonylated iron-sulfur compounds and the synthesis of pyruvate. *Science* **289**, 1337–1340 (2000).
12. M. Preiner *et al.*, A hydrogen-dependent geochemical analogue of primordial carbon and energy metabolism. *Nat. Ecol. Evol.* **4**, 534–542 (2020).
13. K. B. Muchowska *et al.*, Metals promote sequences of the reverse Krebs cycle. *Nat. Ecol. Evol.* **1**, 1716–1721 (2017).
14. K. B. Muchowska, S. J. Varma, J. Moran, Synthesis and breakdown of universal metabolic precursors promoted by iron. *Nature* **569**, 104–107 (2019).
15. M. A. Keller, A. V. Turchyn, M. Ralsler, Non-enzymatic glycolysis and pentose phosphate pathway-like reactions in a plausible Archean ocean. *Mol. Syst. Biol.* **10**, 725 (2014).

Materials and Methods

Model Description. In this study, we formulated a protocell model similar to the one we previously considered to estimate the membrane potentials that can be generated across iron-sulfide membranes in abiotic cells (20). The main goal of this model is to simulate alkaline hydrothermal vent (AHV) conditions on the Early earth. Specifically, the protocell in this model is intended to represent AHV micropores and answer whether they could have harbored early carbon-fixing cycles at the origin of metabolism. We considered an idealized protocell model of AHV micropores. The protocell is a sphere of radius R_c with a semipermeable membrane of thickness d (SI Appendix, Fig. S1D). The membrane is primarily made of iron sulfides possibly mixed with other minerals. Under hydrothermal conditions, similar cellular structures made of iron monosulfide can form when ferrous iron is mixed with alkaline fluids that are rich in HS^- (31). We assume that a simple hypothetical thiol HS-R (e.g., ethane thiol (8)) existed in primitive AHVs that drove the thioesterification steps of first metabolic networks. The interior of the protocell is filled with acidic ocean water ($\text{pH} = 5$), while its outer membrane is exposed to alkaline hydrothermal fluids ($\text{pH} = 9$) (Fig. 1 A and B). Because of this pH gradient, a positive membrane potential $\Delta\psi$ develops across the membrane (20). We refer to the acidic interior of the protocell as the intracellular environment (denoted 'In' in Fig. 2A) and alkaline hydrothermal fluids outside the protocell as the extracellular environment (denoted 'Out' in Fig. 2A). An extensive description of the protocell model is provided in SI Appendix, Model Description.

Fundamental Constraints. We determined the feasibility of first carbon-fixing cycles at the origin of metabolism by solving the species mass-balance equations for all the reactants in the protometabolic network described in the main text (Fig. 1C) subject to fundamental physicochemical constraints of the early Earth (Fig. 1D). In this formulation, steady-state solutions of the species mass-balance equations represent the homeostatic states of the protometabolic network. We then ascertained the stability of steady-state solutions using a linear stability analysis to identify the conditions under which the protometabolic network is self-sustaining. Detailed formulations of the fundamental physicochemical constraints, linear stability analysis, and computational techniques are provided in SI Appendix.

Data, Materials, and Software Availability. All data generated or analyzed during this study and all the codes used for analysis with their description are included in this published article and its [Supplementary Materials](#).

ACKNOWLEDGMENTS. This work was funded by the Novo Nordisk Foundation (Grant No. NNF10CC1016517) and the NIH (Grant No. GM057089).

16. N. Lane, W. F. Martin, The origin of membrane bioenergetics. *Cell* **151**, 1406–1416 (2012).
17. D. W. Deamer, *Assembling Life: How Can Life Begin on Earth and Other Habitable Planets?* (Oxford University Press, 2018).
18. A. Eschenmoser, On a hypothetical generational relationship between HCN and constituents of the reductive citric acid cycle. *Chem. Biodivers.* **4**, 554–573 (2007).
19. E. Camprubi, S. F. Jordan, R. Vasiliadou, N. Lane, Iron catalysis at the origin of life. *IUBMB Life* **69**, 373–381 (2017).
20. A. Akbari, B. O. Palsson, Positively charged mineral surfaces promoted the accumulation of organic intermediates at the origin of metabolism. *PLoS Comput. Biol.* **18**, e1010377 (2022).
21. E. Smith, H. J. Morowitz, Universality in intermediary metabolism. *Proc. Natl. Acad. Sci. U.S.A.* **101**, 13168–13173 (2004).
22. G. D. Cody *et al.*, Geochemical roots of autotrophic carbon fixation: Hydrothermal experiments in the system citric acid, h_2o -(\pm fes)-(\pm nis). *Geochim. Cosmochim. Acta* **65**, 3557–3576 (2001).
23. M. A. Keller, D. Kampjut, S. A. Harrison, M. Ralsler, Sulfate radicals enable a non-enzymatic Krebs cycle precursor. *Nat. Ecol. Evol.* **1**, 1–9 (2017).
24. E. Chevallot-Beroux, J. Gorges, J. Moran, Energy conservation via thioesters in a non-enzymatic metabolism-like reaction network. *Chemrxiv* 2019, <https://chemrxiv.org/engage/chemrxiv/article-details/60c742ec469df4536af4308b>. Accessed 9 July 2019.
25. A. Akbari, J. T. Yurkovich, D. C. Zielinski, B. O. Palsson, The quantitative metabolome is shaped by abiotic constraints. *Nat. Commun.* **12**, 1–19 (2021).
26. R. Alberty, *Thermodynamics of Biochemical Reactions* (John Wiley & Sons, 2005).
27. F. Dyson, *Origins of Life* (Cambridge University Press, 1999).
28. E. Smith, H. J. Morowitz, *The Origin and Nature of Life on Earth: The Emergence of the Fourth Geosphere* (Cambridge University Press, 2016).
29. R. J. Mayer, H. Kaur, S. A. Rauscher, J. Moran, Mechanistic insight into metal ion-catalyzed transamination. *J. Am. Chem. Soc.* **143**, 19099–19111 (2021).
30. S. Scintilla *et al.*, Duplications of an iron-sulphur tripeptide leads to the formation of a protoferredoxin. *Chem. Commun.* **52**, 13456–13459 (2016).
31. M. J. Russell, A. J. Hall, D. Turner, In vitro growth of iron sulphide chimneys: Possible culture chambers for origin-of-life experiments. *Terra Nova* **1**, 238–241 (1989).